Ultrasound in Med. & Biol., Vol. 47, No. 5, pp. 1219–1226, 2021

0301-5629/$ - see front matter

https://doi.org/10.1016/j.ultrasmedbio.2021.01.019

● *Original Contribution*

MULTIPARAMETRIC ULTRASOUND EVALUATION OF THE THYROID: ELASTOGRAPHY AS A KEY TOOL IN THE RISK PREDICTION OF UNDETERMINED NODULES (BETHESDA III AND IV)—HISTOPATHOLOGICAL CORRELATION

Pedro H.M. Moraes,* Marcelo Straus Takahashi,* Felipe A.B. Vanderlei,†
Marcelo V. Schelini,* Danielle A. Chacon,‡
Marcos Roberto Tavares,† and Maria Cristina Chammas*

* Institute of Radiology, Hospital das Clínicas, School of Medicine, University of São Paulo, São Paulo, SP, Brazil; † Head and Neck Surgery Department, Hospital das Clínicas, School of Medicine, University of São Paulo, São Paulo, SP, Brazil; and ‡ Pathology Department, Hospital das Clínicas, School of Medicine, University of São Paulo, São Paulo, SP, Brazil

(*Received* 3 *September* 2020; *revised* 18 *December* 2020; *in final from* 18 *January* 2021)

Abstract—The purpose of this study was to select thyroid nodules most at risk for malignancy among those cytologically undetermined by fine-needle aspiration biopsy (FNAB), using B-mode, color duplex Doppler and 2-D shear wave shear wave elastography (2-D-SWE). This was a prospective diagnostic accuracy study with 62 Bethesda III/IV nodules according to FNAB (atypia/follicular lesion of undetermined significance or follicular neoplasia/Hürthle cell neoplasm). Ultrasonography (US) data were compared with resection histologic results, revealing 35 of 62 benign nodules (56.4%) and 27 of 62 carcinomas (43.6%). Conventional US was uses to evaluate nodule echogenicity, dimensions, contours, presence of halo and microcalcifications. Doppler US was used to assess the vascularization (exclusively or predominantly peripheral or central) and mean resistance index of three nodule arteries. Elastography was used to evaluate the nodule elastographic pattern; mean nodule deformation index; deformation ratio between nodule and adjacent thyroid parenchyma; and mean deformation ratio between nodule and pre-thyroid musculature (MDR). Statistical analysis included χ^2, Fisher's exact, Student's *t*, Mann–Whitney tests and multivariable analysis by multiple logistic regression. Areas under the receiver operating characteristic curves (AUC-ROCs) were used for accuracy analysis. Fifty-eight participants (54.7 ± 14.0 y, 51 women) were studied. The parameters that were statistically significant to the univariate analysis were hypoechogenicity, nodule diameter greater than width and all parameters analyzed from Doppler and elastography. Multivariate analysis revealed that the MDR (in kPa) was the best parameter for risk analysis of indeterminate nodules. Nodules with MDRs >1.53 exhibited a greater chance of malignancy (AUC-ROC = 0.98). We conclude that 2-D-SWE is able to select malignant nodules among those cytologically indeterminate, thus avoiding unnecessary surgery in these cytologic groups. (E-mail: pedrohenrique.mmoraes@gmail.com) © **2021 World Federation for Ultrasound in Medicine & Biology. All rights reserved.**

Key Words: **Ultrasound, Indeterminate cytology, Shear-wave elastography, Thyroid nodules, Histology correlation.**

INTRODUCTION

With the advent and improvement of ultrasound (US), the percentage of thyroid nodules diagnosed in the general population has grown, reaching up to 50% in the population over 40 y of age (Topliss 2004; Guth et al. 2009). Fine-needle aspiration biopsy (FNAB) with subsequent cytologic analysis is used to identify nodules with a higher risk of malignancy that should be referred for surgery and to exclude thyroid nodules that should be followed with periodic US or only clinically. FNAB of all nodules identified on US is unfeasible. Therefore, criteria for increased risk were established by conventional US (B-mode): nodular hypo-echogenicity (highly hypoechogenic nodules are most associated with malignancy), absence of hypo-echogenic peripheral halo, presence of microcalcifications, anteroposterior diameter larger than latero-lateral diameter, irregular contours and poorly defined margins (Grant et al. 2015; Haugen et al. 2016). Other criteria are nodule vascularization patterns and

Address correspondence to: Pedro Henrique De Marqui Moraes. Av. Dr. Enéas de Carvalho Aguiar, 255— 3rd floor, Cerqueira Cesar, São Paulo SP, Brazil, 05403-001. E-mail: pedrohenrique.mmoraes@gmail.com

artery resistance indexes by Doppler (Chammas et al. 2005; De Nicola et al. 2005; Iared et al. 2010). US assessment is controversial because it depends on the criteria used, the sensitivity of the equipment and the operator's experience with the method in question.

FNAB may classify thyroid nodules as with indeterminate cytology: atypia of undetermined significance (follicular lesion of undetermined significance), which is a very heterogeneous group (Bethesda III and follicular neoplasms or Hürthle cell follicular neoplasm [Bethesda IV]) (Cibas and Ali 2017). The difficulty of differential diagnosis is due, in addition to the cytologic similarity, to the impossibility of verifying in the FNAB if there is invasion of vessels and/or the capsule, which is the most reliable criterion in malignancy. Bethesda III and IV diagnosis are made in 10%−30% of thyroid nodule FNABs, resulting in approximately 20% malignancy at the final histologic analysis (Goellner et al. 1987; Chow et al. 2001; Smith et al. 2005). Eighty percent of Bethesda III and IV surgically resected thyroid nodules are benign.

To reduce the number of participants requiring surgical intervention, with all the comorbidities and associated costs (Cibas and Ali 2017), we proposed this study, in which we evaluate whether and which parameters of conventional US (B-mode and Doppler) and 2-D-shear wave elastography (SWE) can distinguish nodules at higher risk for malignancy from those with indeterminate FNAB (Bethesda class III and IV cytology), comparing these parameters with histologic analysis after surgical resection (reference standard). This is the first study to compare a complete parameter set of these three US techniques.

METHODS

Study participants

Eighty-five participants were consecutively recruited within the inclusion criteria: patients of both sexes and all ages, with thyroid nodules cytologically Bethesda III and IV after FNAB and in the queue for surgical resection. Sixty-two thyroid nodules (in 3 participants, 2 nodules were analyzed) were studied. FNAB indicated that 35 of 62 nodules (56.4%) were of atypia of undetermined significance (only nodules with repeated atypia of undetermined significance in at least 2 FNABs were included and nodules with suspicious US and/or clinical characteristics) and 27 of 62 (43.6%) were follicular neoplasms. These nodules were candidates for surgical treatment for histologic distinction between benign or malign lesions.

The Research Ethics Committee for Research Project (CAPPesq) approved this study, which complies with the Declaration of Helsinki, and participants were enrolled after signing the consent form. The exclusion criteria were presence of two or more superposed nodules, nodules with anterior calcification or large cystic areas (factors that, in addition to impairing the assessment of posterior nodule contours in B-mode and Doppler, hamper acoustic radiation force impulse and shear wave propagation, producing artifacts in the elastogram) and participants without surgical indication or condition. The statistical analysis was done with data from 58 of the 85 participants on whom surgery was performed. The decision on whether surgery should be executed was made by a head and neck surgery team based on previous US findings, FNAB and clinical history. The result of this study was not provided to the head and neck surgery team and has not influenced the surgical approach.

The sample size was calculated with the primary objective of estimating the performance of the parameters studied in discriminating the nodules at higher risk for malignancy. For an estimated area under the receiver operating characteristic curve (AUC-ROC) of at least 0.8, α of 0.05 and power of 0.80, considering a null hypothesis of AUC-ROC 0.6, we estimated that a sample size of 56 patients would be needed.

Surgeries were performed from December 2016 to July 2018 in our institution. The average interval between US and surgery was approximately 2 wk. Fifty-one (87.9%) participants were women, and age ranged from 24−80 y.

Each nodule was evaluated using the GE Logiq E9 (GE Healthcare, Milwaukee, WI, USA) with 2-D-SWE software. A linear 12- to 15-MHz transducer was used for B-mode and color duplex Doppler, and another with 9 MHz for elastography. The examinations were performed by two physicians with at least 3 y elastography experience. The Bethesda class III or IV diagnosis was not provided to reduce bias. Agreement on elastogram score was greater than 90% between the two performers (56 of 62 nodules). In 6 cases, the final score was agreed on after a joint review of the recorded images.

B-Mode ultrasound

The following parameters were analyzed and detailed in the Supplementary Data (online only): nodule dimensions and the ratio of the anteroposterior diameter to the transverse diameter; nodule echogenicity; peripheral halo; and calcification.

Color Doppler (conventional and amplitude)

Doppler analysis of blood flow was classified according to blood flow patterns: I = absence of signal; II = exclusively perinodular; III = perinodular more evident than central; IV = marked central and less significant perinodular; V = exclusively central (Chammas et al. 2005).

Pulsed Doppler

Arterial blood flow to the nodules was quantified by spectral analysis. The same equipment configurations used for qualitative analyses were applied by adding a sample volume of 2 mm. The duplex parameter obtained

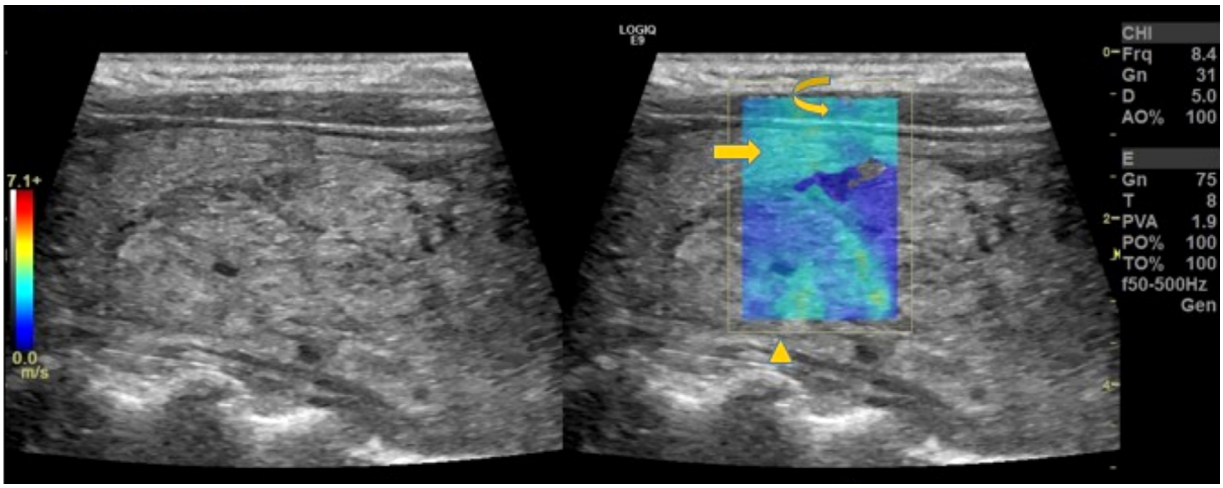

Fig. 1. Two-dimensional shear wave elastography (2-D-SWE) acquisitions along the longitudinal plane: B-mode image on the left and overlaid elastogram on the right. Healthy thyroid tissue is represented by homogeneous *blue/green* (*straight arrow*). The capsule and adjacent connective tissues, as well as the cervical muscles, are represented in *blue*; there may be *yellow dots* (*curved arrow*). The field of view (*yellow box containing elastogram*) should be the maximum diameter that allows the inclusion of all or most of the evaluated nodule and should include part of the pre-thyroid muscles and thyroid tissue adjacent to the nodule (*arrowhead*).

was the resistance index, and the average of three nodule indexes was calculated (Chammas et al. 2005).

2-D-Shear wave elastography

In the 2-D-SWE image, the elastogram is formed by a color scale in a field of view, superimposed on a B-mode image ranging from blue (highly elastic soft tissues) to red (harder components with minor deformity) (Fig. 1). We proposed an elastogram classification considering nodule stiffness, ranging from pattern 1 (100% blue, completely soft) to 4 (100% red, completely hardened) (Fig. 2). Further details regarding elastographic acquisitions are provided in the Supplementary Data (online only).

After elastogram analysis, a spherical region of interest (ROI) with adjustable diameter was selected for measurement of deformation indexes of nodules, thyroid parenchyma and pre-thyroid muscle. The ROI should include all or most of the nodule that fits in the elastogram (the maximum field of view diameter allowed by the manufacturer is 3.0×2.0 cm). If the nodule was larger than the field of view, the measurements were made in different areas. ROIs in this study ranged from 0.6 to 2.0 cm (maximum allowed by the manufacturer). Deformation indexes were calculated both in meters/second and kilopascals (Young's modulus), further detailed in the Supplementary Data (online only) (Fig. 3). Two areas on the same elastogram were used to calculate two deformation ratios: (i) nodule/thyroid deformation ratio (TDR); (ii) nodule/muscle deformation ratio (MDR). For each of the five elastograms selected, a nodule SWE index, a thyroid parenchyma SWE index and a pre-thyroid musculature SWE index were calculated. Ten TDRs and 10 MDRs were produced per nodule, five using values in meters/second and five in kilopascals.

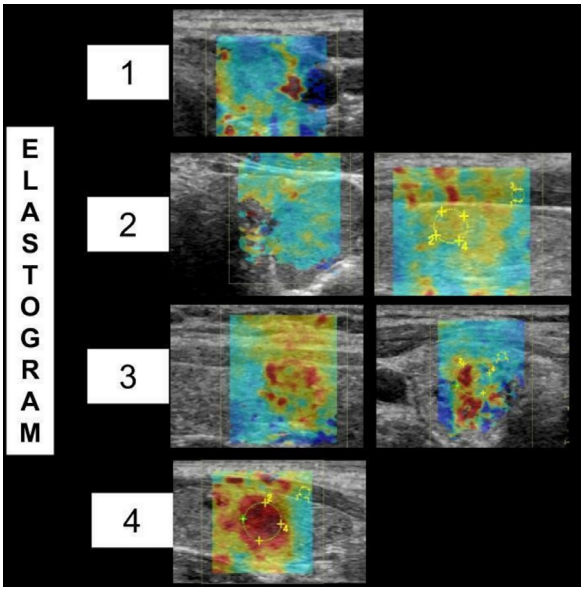

Fig. 2. Elastogram classification according to nodule stiffness percentage. From left to right: B-mode image, overlaid elastogram and schematic representation of elastogram pattern. Pattern 1 100% *blue* (completely soft); pattern 2 *yellow/red* in up to 49% of the nodule or only *yellow* in most of the nodule (without red dots); pattern 3 *yellow/red* $\geq$50% of the nodule; pattern 4 100% *red* (completely hard).

Pathologic anatomy

The cytologic diagnosis was performed by three pathologists with at least 5 y experience. Cytologic diagnoses

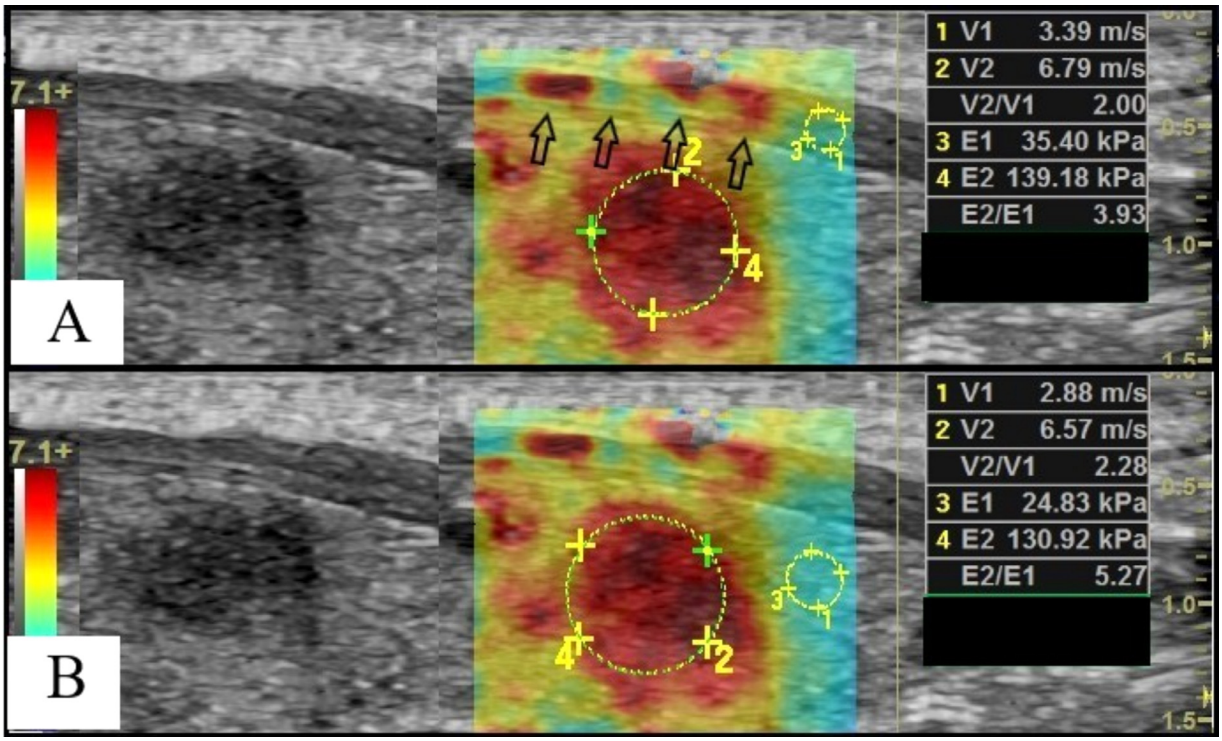

Fig. 3. Field-of-view choice for deformation index determination. Longitudinal plane B-mode image on the left, and overlaid elastogram on the right. Yellow spherical regions of interest (ROIs) for the measurement of nodule deformation index (2 and 4) and of pre-thyroid muscle (a) or thyroid parenchyma (b) (1 and 3). The measured indexes, as well as the deformation ratios in meters/second (*V*) and Young's modulus (*E*, kPa) appear on the right. The area anterior to the thyroid (*black arrows*) should be avoided to obtain the muscle SWE index as the isthmus is bulging out structures anterior to the thyroid (proximal field artifacts).

followed the 2017 Bethesda system for the Thyroid Cytopathology Report (Cibas and Ali 2017). Surgeries were performed by the Head and Neck Surgery Division, Hospital das Clínicas of São Paulo, and the Cancer Institute of São Paulo. The histologic diagnosis was made by pathologists from the Department of Anatomic Pathology with experience in head and neck pathology.

Statistical analysis

Categorical variables were described by absolute and relative frequencies and compared using the χ^2 test or Fisher's exact test. Continuous variables were evaluated for normality through graphical methods, skewness and kurtosis values. Data with normal distributions were described by means and standard deviations and compared using Student's *t*-test, and non-normal data were expressed as medians and quartiles and compared with the Mann–Whitney *U*-test. No data were lost.

Predictors of malignancy were identified by multivariable analysis further detailed in the Supplementary Data (online only). Discrimination was assessed with the AUC-ROC, compared with the DeLong test and the integrated discrimination improvement index, a measure of the difference in probability of malignancy between benign and malignant histology groups as predicted by each model.

Tests were two-tailed, and final values of $p < 0.05$ were indicated significance.

RESULTS

The study was carried out with 58 participants (51 women), aged 54.7 ± 14.0 y (mean ± standard deviation [SD]). Four participants had two nodules each, totaling 62 nodules (Table 1).

The histologic analysis after surgery revealed that 35 of 62 nodules (56.4%) were benign and 27 of 62 nodules (43.6%) were carcinomas. Of the 33 nodules diagnosed by FNAB as Bethesda III, 20 were benign and 15 were malignant (2 follicular thyroid carcinomas, 9 papillary carcinomas, follicular variant and 4 differentiated thyroid carcinomas). As for the 27 nodules classified by FNAB as Bethesda IV, 15 were benign and 12 were malignant (3 follicular thyroid carcinomas, 4 papillary carcinomas, follicular variant, 4 differentiated thyroid carcinomas and 1 oncocytic follicular thyroid carcinoma).

Table 1. General sample characterization according to histologic finding

Variable	General (62)	Malignant		*p* Value
		No (35)	Yes (27)	
Age	54.7 ± 14.0	56.2 ± 14.3	52.8 ± 13.7	0.35
Female	55 (88.7)	30 (85.7)	25 (92.6)	0.46
B-mode				
Hypo-echogenic	29 (46.8)	10 (28.6)	19 (70.4)	0.001
Size				
Anteroposterior/transverse (cm)	0.81 (0.67−0.95)	0.79 (0.65−0.92)	0.85 (0.71−1.14)	0.036
Volume (cm^3)	3.17 (1.21−16.92)	2.25 (0.97−6.99)	7.16 (1.87−49.82)	0.064
Doppler				
Resistivity index	0.59 ± 0.09	0.58 ± 0.08	0.60 ± 0.10	0.46
Vascularization pattern				<0.001
II	1 (1.6)	1 (2.9)	0 (0.0)	
III	39 (62.9)	34 (97.1)	5 (18.5)	
IV	19 (30.6)	0 (0.0)	19 (70.4)	
V	3 (4.8)	0 (0.0)	3 (11.1)	
Elastography pattern				<0.001
I	3 (4.8)	3 (8.6)	0 (0.0)	
II	33 (53.2)	29 (82.9)	4 (14.8)	
III	18 (29.0)	3 (8.6)	15 (55.6)	
IV	8 (12.9)	0 (0.0)	8 (29.6)	
Nodule velocity (m/s)	3.58 ± 0.96	3.09 ± 0.65	4.22 ± 0.93	<0.001
Nodule elastography (kPa)	43.93 ± 23.76	31.88 ± 12.28	59.55 ± 26.05	<0.001
TDR (m/s)	1.33 ± 0.38	1.10 ± 0.25	1.62 ± 0.30	<0.001
TDR (kPa)	1.80 ± 0.80	1.33 ± 0.57	2.40 ± 0.63	<0.001
MDR (m/s)	1.24 ± 0.28	1.06 ± 0.16	1.47 ± 0.21	<0.001
MDR (kPa)	1.58 ± 0.61	1.17 ± 0.30	2.11 ± 0.50	<0.001

The categorical variables are presented as the n (%), and the continuous variables, as the mean ± standard deviation, except size (median and quartiles).

TDR = thyroid deformation ratio (nodule deformation SWE index/thyroid deformation SWE index); MDR = muscle deformation ratio (nodule deformation SWE index/ muscle deformation SWE index); SWE = shear wave elastography.

Univariate analysis

B-mode ultrasound. The longitudinal size ranged from 0.8−10.0 cm; the average tumor size was 3.7 cm for benign and 2.7 cm for malignant tumors. Benign nodules had an average anteroposterior/transverse axis diameter ratio of 0.79 (95% confidence interval [CI]: 0.65−0.92) and malignant nodules of 0.85 (95% CI: 0.71−1.14) by B-mode US ($p = 0.036$). ROC analysis provided an AUC of 0.65 (95% CI: 0.512−0.800) (Table 1).

Regarding echogenicity, 29 of 62 nodules (46.8%) were hypo-echogenic. Of these, 19 of 29 (65.5%) had malignant histology. Therefore, hypo-echogenicity was considered significant evidence of malignancy ($p = 0.001$).

Duplex Doppler. Predominantly central blood flow and exclusively central blood flow (Chammas et al. 2005) were observed in 21 of 62 nodules (33.8%). All 21 of these were malignant on final histology. Statistical analysis revealed a correlation between vascularization patterns II to V and malignancy ($p < 0.001$) (Table 1).

Elastography. The elastogram pattern (Table 1) based on nodule stiffness differed between benign and malignant nodules ($p < 001$) and had the following results: pattern I in 3 of 62 nodules (5%), all benign; pattern II in 33 of 62 nodules (53.2%), of which 29 of 33 (87.8%) were benign; pattern III in 18 of 62 nodules (29%), 15 of 18 (83.3%) malignant; pattern IV in 8 of 62 nodules (12.9%), 100% malignant. Twenty-three (88.5%) of the 27 malignant nodules had pattern 3 or 4. Patterns 3 and 4 were correlated with 68% and 108% malignancy, respectively ($p = 0.000$, sensitivity = 80.8% and specificity = 88.9%).

Univariate analysis revealed a correlation ($p < 0.001$) between nodule stiffness by SWE index and malignancy. The mean (±SD) for benign lesions was 3.09 m/s (0.65 m/s), and for malignant lesions, 4.22 m/s (0.93 m/s). ROC curve analysis provided an AUC of 0.866 (95% CI: 0.744−0.958). Twenty-eight of the nodules had an SWE index >3.62 m/s. Of these, 22 of 28 (78.5%) were malignant. At a cutoff value of 3.62 m/s, a sensitivity of 81.5% and specificity of 82.9% were obtained. The results using the mean nodule SWE index in Young's modulus (kPa) were also significant ($p < 0.001$): the mean (±SD) for benign lesions was 31.88 kPa (12.28 kPa) and for malignant lesions, 59.55 kPa (26.05 kPa; ROC-AUC = 0.863, 95% CI: 0.771−0.955). With a cut-off value of 42.03 kPa, sensitivity was 81.5% and specificity, 80.0% (Tables 1 and 2).

Table 2. Elastography parameter discrimination accuracy

Parameter	Cutoff	Sensitivity	Specificity	AUC-ROC	SE	95% CI	*p* Value
Nodule velocity	3.625	81.5	82.9	0.87	0.047	0.774−0.958	<0.001
Nodule elastography	42.035	81.5	80.0	0.86	0.047	0.771−0.955	<0.001
TDR (m/s)	1.360	81.5	91.3	0.90	0.038	0.831−0.978	<0.001
TDR (kPa)	1.815	88.9	91.3	0.91	0.039	0.831−0.986	<0.001
MDR (m/s)	1.225	88.9	94.3	0.97	0.019	0.928−1.000	<0.001
MDR (kPa)	1.530	92.6	94.3	0.98	0.016	0.945−1.000	<0.001

AUC-ROC = area under the receiver operating characteristic curve; SE = standard error; CI = confidence interval; TDR = thyroid deformation ratio (nodule deformation SWE index/thyroid deformation SWE index); MDR = muscle deformation ratio (nodule deformation SWE index/muscle deformation SWE index).

The deformation ratio between nodule and pre-thyroid musculature (MDR), with values calculated in kilopascals, was higher in malignant nodules ($p = 0.000$). The mean relationship between benign lesions and pre-thyroid muscles was 1.17 (±0.30), and that for malignant lesions, 2.11 (± 0.50; ROC-AUC = 0.976, 95% CI: 0.945−1.00). Twenty-seven nodules had MDRs >1.53 (in kPa). Of the 27, 25 (92.6%) were malignant. At an MDR cutoff 1.53, sensitivity was 92.6% and specificity 94.3%, VVP was 92.7% and VPN 99.9%. The MDR for values in meters/second, as well as the relationship between the nodule and the adjacent thyroid parenchyma (TDR), were also higher in malignant nodules, with slightly lower values, as outlined in Tables 1 and 2.

Multivariable analysis

Multivariable analysis included the following parameters with $p < 0.10$ in the univariable analysis: nodule echogenicity, anteroposterior/transverse diameter, Doppler vascularization pattern (Chammas et al. 2005) and the variables obtained by elastography. The variable chosen for multivariable analysis was the MDR (in kPa) because it is more objective, has lower variability and is easy to calculate (with lower selection bias) (Table 3). MDR and high-risk vascularization pattern (IV and V) were the statistically significant parameters in the multivariable analysis with $p = 0.002$ and 0.005, respectively (Table 4).

The MDR was the best parameter for predicting risk of malignancy of cytologically indeterminate nodules. For each increased unit of the ratio between the nodule SWE index and MDR in kilopascals, the probability of finding malignant histology rises 354.25 times (Table 4).

DISCUSSION

This research was aimed at analyzing ultrasonographic, duplex Doppler and elastographic parameters to search for the best criteria to select the malignant nodules among those cytologically indeterminate (Bethesda III and IV). These parameters were compared with the histologic outcome after surgical resection as a standard. On multivariable analysis, the best predictor for malignancy was the deformation ratio between the nodule and the pre-thyroid musculature (MDR).

Unlike the values reported in the literature (Cibas and Ali 2017), we obtained a high percentage of carcinomas (27 of 62). This may be owing to the selection of the Bethesda III group, which had at least two FNABs with repeated atypia of indeterminate significance. Additionally, these participants had suspicious clinical and/or US findings for malignancy. In the Bethesda IV group, there were a larger number of Hürthle cell follicular neoplasms (21 of 27, 78%) than found in other studies (6%−48%, with an average risk of 16% [Bongiovanni et al. 2012] and 15%−45% for participants with Hürthle cell carcinoma [Cibas and Ali 2017]).

Table 3. Elastography parameter discrimination accuracy

Variable	AUC-ROC	SD error	*p* value	95% CI	
				Inferior limit	Superior limit
Nodule velocity	0.866	0.047	0.000	0.774	0.958
Nodule elastography	0.863	0.047	0.000	0.771	0.955
TDR (m/s)	0.904	0.038	0.000	0.831	0.978
TDR (kPa)	0.908	0.039	0.000	0.831	0.986
MDR (m/s)	0.966	0.019	0.000	0.928	1.000
MDR (kPa)	0.976	0.016	0.000	0.945	1.000

All parameters shown are predictors of malignancy, with MDR (kPa) having the highest AUC.

AUC-ROC = area under the receiver operating characteristic curve; SD = standard deviation; CI = confidence interval; TDR = thyroid deformation ratio (nodule deformation SWE index/thyroid deformation SWE index); MDR = muscle deformation ratio (nodule deformation SWE index/muscle deformation SWE index).

Table 4. Independent predictors and probability model of malignancy

Variable	Coeff.	SE	95% CI	OR	*p* value
Independent predictors of malignancy					
Hypo-echogenic nodule	0.80	1.27	−2.04 to 3.83	2.23	0.549
Size (anteroposterior)* (each unit)	1.12	5.62	−9.30 to 27.56	3.06	0.846
High risk vascularization pattern (pattern IV or V)	3.55	1.65	0.95−8.53	34.81	0.005
MDR (kPa) (each unit)	5.16	2.04	1.67−10.67	174.16	0.002
Probability model for prediction of malignancy					
High-risk vascularization pattern (pattern IV or V)	4.05	1.71	1.47−9.06	57.40	0.001
MDR (kPa) (each unit)	5.87	2.08	2.46−11.61	354.25	<0.001

Coeff = coefficient; SE = standard error; OR = odds ratio; CI = confidence interval; MDR = muscle deformation ratio (nodule deformation SWE index/muscle deformation SWE index).

* Logarithmic transformation for normalization.

The idea of correlating the elasticity of the nodule with that of the pre-thyroid musculature is a different and promising proposal that suppresses possible bias in the presence of abnormal thyroid parenchyma (*e.g.,* thyroiditis). There are no studies in the literature on the relationship between elasticity of pre-thyroid muscles and elasticity of exclusively follicular nodules. Kim et al. (2013) calculated the elasticity ratios between all types of thyroid nodules (not only follicular ones) before FNAB and pre-thyroid muscles and found no statistically significant difference between malignant and benign thyroid nodules. They assumed that the reasons for this were that muscle width and stiffness differed between participants and did not standardize these factors for comparison. Our study, on the other hand, found a 354.25-fold increased risk of malignancy for each increased unit of the ratio between the nodule SWE index and the muscle SWE index calculated in kilopascals (MDR) (coefficient = 5.87; 95% CI: 2.46−11.61; $p < 0.001$). Follicular-patterned nodules that had a ratio >1.53 had a high risk of malignancy (sensitivity = 92.6%, specificity = 94.3%). We attributed this divergence to the fact that all elastograms in our study had a standardized measurement: they were performed in the longitudinal plane, and with a slight extension of the participant's neck. In addition, the muscle region immediately before the nodule was avoided. These precautions have helped to avoid areas of hyperextension that erroneously increase the muscle deformation ratio.

Ciledag et al. (2012) suggested that the musculature could be used for this relationship in cases of diffuse thyroid parenchymal involvement, using semiquantitative elastographic measurements of SE. Contrary to our study, no significant difference was found in relation to muscle or thyroid parenchyma. In our study, it was observed that the ratio between nodule elasticity and pre-thyroid musculature elasticity was statistically better than the same relationship with the parenchyma. This may be related to distortions caused by the large number of areas of thyroiditis and/or fibrosis observed in the general population.

The multivariable analysis of the present study revealed that the MDR is the most significant predictor of malignancy in nodules with indeterminate cytology in FNAB. The diagnostic sensitivity and specificity for MDR >1.53 are 92.6% and 94.3%, respectively.

There may have been undetected bias in selecting participants for surgery or recruitment; however, the prospective and blinded nature of the study certainly minimized the possibility of this selection bias. Known confounding factors of elasticity values such as breathing and pre-compression were reduced by standardizing the participant's position with a slight neck hyperextension, as well as the positioning of the elastographic regions of interest in our study. Nodules with cystic areas and coarse and eggshell calcifications can generate elastogram artifacts and were avoided in elastogram acquisitions in our study. Another possible limitation of our study is subjectivity in the classification of nodules based on elastographic patterns. Thus, it is interesting to pursue this line of research by performing inter-observer as well as intra-observer analysis.

CONCLUSIONS

Various ultrasound parameters were found to be helpful in risk prediction in cytologically indeterminate thyroid nodules (Bethesda III and IV). By univariate analysis, these included hypo-echogenicity, nodule diameter greater than width and all parameters analyzed from Doppler and elastography. Multivariate analysis revealed that 2-D-SWE had the best sensitivity, specificity and accuracy in predicting malignancy risk. Furthermore, elastography is a very reproducible method, which does not depend, for example, on device pre-set adjustments, as occurs in the Doppler evaluation. Compared with that of pre-thyroid muscles, the elastography pattern using the nodule deformation ratio proved to be a valuable tool in the analysis of cytologically indeterminate nodules, capable of selecting those with the highest risk of malignancy.

Acknowledgments—We acknowledge the work of the Head and Neck Surgery Division, Hospital das Clínicas of São Paulo, who helped us by performing the surgeries on the selected participants.

This Project was partially supported by funds from GE Healthcare, who also lent us equipment. This funding agency had no involvement in study design; in the collection, analysis and interpretation of data; in the writing of the article; and in the decision to submit the article for publication.

Conflict of interest disclosure—Our institution had partial funding from GE for this research.

SUPPLEMENTARY MATERIALS

Supplementary material associated with this article can be found in the online version at doi:10.1016/j.ultrasmedbio.2021.01.019.

REFERENCES

Bongiovanni M, Crippa S, Baloch Z, Piana S, Spitale A, Pagni F, Mazzucchelli L, Di Bella C, Faquin W. Comparison of 5-tiered and 6-tiered diagnostic systems for the reporting of thyroid cytopathology. Cancer Cytopathol 2012;120:117–125.

Chammas MC, Gerhard R, de Oliveira IR, Widman A, de Barros N, Durazzo M, Ferraz A, Cerri GG. Thyroid nodules: Evaluation with power Doppler and duplex Doppler ultrasound. Otolaryngol Head Neck Surg 2005;132:874–882.

Chow LS, Gharib H, Goellner JR, van Heerden JA. Nondiagnostic thyroid fine-needle aspiration cytology: Management dilemmas. Thyroid 2001;11:1147–1151.

Cibas ES, Ali SZ. The 2017 Bethesda system for reporting thyroid cytopathology. J Am Soc Cytopathol 2017;6:217–222.

Ciledag N, Arda K, Aribas BK, Aktas E, Kose SK. The utility of ultrasound elastography and MicroPure imaging in the differentiation of benign and malignant thyroid nodules. AJR Am J Roentgenol 2012;198:W244–W249.

De Nicola H, Szejnfeld J, Logullo AF, Wolosker AM, Souza LR, Chiferi V, Jr. Flow pattern and vascular resistive index as predictors of malignancy risk in thyroid follicular neoplasms. J Ultrasound Med 2005;24:897–904.

Goellner JR, Gharib H, Grant CS, Johnson DA. Fine needle aspiration cytology of the thyroid, 1980 to 1986. Acta Cytol 1987;31:587–590.

Grant EG, Tessler FN, Hoang JK, Langer JE, Beland MD, Berland LL, Cronan JJ, Desser TS, Frates MC, Hamper UM, Middleton WD, Reading CC, Scoutt LM, Stavros AT, Teefey SA. Thyroid ultrasound reporting lexicon: White Paper of the ACR Thyroid Imaging, Reporting and Data System (TIRADS) Committee. J Am Coll Radiol 2015;12:1272–1279.

Guth S, Theune U, Aberle J, Galach A, Bamberger CM. Very high prevalence of thyroid nodules detected by high frequency (13 MHz) ultrasound examination. Eur J Clin Invest 2009;39:699–706.

Haugen BR, Alexander EK, Bible KC, Doherty GM, Mandel SJ, Nikiforov YE, Pacini F, Randolph GW, Sawka AM, Schlumberger M, Schuff KG, Sherman SI, Sosa JA, Steward DL, Tuttle RM, Wartofsky L. 2015 American Thyroid Association management guidelines for adult patients with thyroid nodules and differentiated thyroid cancer: The American Thyroid Association guidelines task force on thyroid nodules and differentiated thyroid cancer. Thyroid 2016;26:1–133.

Iared W, Shigueoka DC, Cristofoli JC, Andriolo R, Atallah AN, Ajzen SA, Valente O. Use of color Doppler ultrasonography for the prediction of malignancy in follicular thyroid neoplasms: Systematic review and meta-analysis. J Ultrasound Med 2010;29:419–425.

Kim H, Kim JA, Son EJ, Youk JH. Quantitative assessment of shear-wave ultrasound elastography in thyroid nodules: Diagnostic performance for predicting malignancy. Eur Radiol 2013;23:2532–2537.

Smith J, Cheifetz RE, Schneidereit N, Berean K, Thomson T. Can cytology accurately predict benign follicular nodules? Am J Surg 2005;189:592–595.

Topliss D. Thyroid incidentaloma: The ignorant in pursuit of the impalpable. Clin Endocrinol (Oxf) 2004;60:18–20.